Shahrood University of Technology
Iranian Society of Mining Engineering (IRSME)
Journal of Mining and Environment (JME)
journal homepage: www.jme.shahroodut.ac.ir
THOMSON REUTERS
Vol. 10, No. 1, 2019, 271-286.
DOI: 10.22044/jme.2019.7622.1618

Assessment of an ore body internal dilution based on multivariate geostatistical simulation using exploratory drill hole data

I. Masoumi[1], G.R. Kamali[1], and O. Asghari[2*]

1. Department of Mining Engineering, Shahid Bahonar University of Kerman, Kerman, Iran
2. Simulation and Data Processing Laboratory, School of Mining Engineering, College of Engineering, University of Tehran, Tehran, Iran

Received 3 November 2018; received in revised form 31 December 2018; accepted 3 January 2019

Keywords

Internal Dilution

Geostatistical Simulation

Sequential Indicator Simulation

Minimum/Maximum Auto-Correlation Factors

Gohar Zamin Iron Ore Mine

Abstract

Dilution can best be defined as the proportion of waste tonnage to the total weight of ore and waste in each block. Predicting the internal dilution based on geological boundaries of waste and ore in each block can help engineers to develop more reliable long-term planning designs in mining activities. This paper presents a method to calculate the geological internal dilution in each block and to correct the ultimate grade of each geological block according to the internal dilution values that have already been calculated for each one of them. In this regard, the input data is first indexed based on the lithological logs of drill holes. The occurrence probabilities of ore and waste in each block are calculated via 100 realizations using the sequential indicator simulation. Dilution is computed as the ratio of waste rock tonnage to the total tonnage of ore and waste. Furthermore, joint simulation of the continuous variables is performed for each mining block using the minimum/maximum auto-correlation factors. In the next step, for each block, the final grade variables including iron and iron oxide are computed by considering the calculated internal dilution. These analyses are applied to the Gohar Zamin iron ore deposit, and the actual internal dilution calculated based on the lithological logs of blast holes is compared with the same values obtained based on the proposed method in each block. The results obtained were found to be satisfactory.

1. Introduction

Calculating the internal dilution based on geological boundaries in each block and accurate assessment of grade for each geological block according to its internal dilution has a significant role in devising a more optimal mine production plan (schedule), dump management, and controlling plant feed grade variations. Along the ore-waste boundaries, dilution can reduce the ore grade to such a degree that it is no longer economical for feeding into the processing plant. Dilution also increases the total tonnage of extracted rock due to the higher ratio of waste to ore, which leads to a rise in the extraction and processing costs. Consequently, the mine lifespan increases, while NPV and the return on investment (ROI) decrease. Accordingly, several models (e.g. analytical, empirical, numerical, analytical-empirical) have been presented in the literature for assessing dilution [1-7]. These models are chosen and utilized according to the mining method and other operational parameters in each case. In [8], a geometrical model has been proposed that is applicable to open-pit mines and is based upon calculating external boundaries of the deposit for each level; other studies have reviewed several analytical-empirical models previously introduced [9-14]. In [15], the influence of different types of risk (i.e. environmental, economic, technical, and environment) on dilution for several mines in Iran, namely Sarcheshmeh open-pit mine, Golgohar iron ore mine, and Moeil iron ore mine has been investigated. Most of the previous studies have considered the exploitation and operational

Corresponding author: o.asghari@ut.ac.ir (O. Asghari).

parameters such as blast hole pattern, equipment type, and operational methods in order to assess dilution. However, up to the present time, there is no model for assessing the internal dilution and grade control based on geological data and rock type, a key factor in long-term mine planning. Obviously, a reliable model for grade estimation that considers the internal dilution factor of each block could help mitigate uncertainties, predict production variables more accurately, and manage the plant feeding process more efficiently.

The geostatistical methods are robust tools for evaluating mineral resources, and are able to reproduce the spatial relationships between different variables. These methods, in both the conditional and non-conditional versions, have been extensively used to simulate complex structures [16]. Moreover, the algorithms of different geostatistical modeling approaches are either object-based or pixel-based. The foremost examples of pixel-based geostatistical methods are sequential indicator simulation (SIS) [17, 18], truncated Gaussian simulation (TGS) [19, 20], and pluri-Gaussian simulation (PGS) [21, 22]. The SIS method has found more applications in geological modeling thanks to its simplicity and flexibility. In order to model the geological structures, rock facies, sedimentary layers, and aquifers, one can employ geostatistical categorical variables using SIS [23-25].

Multivariate modeling of different mineralization controlling factors has been widely used in mineral exploration in order to improve the evaluation of ore deposits. It is very important to ensure the accuracy of joint simulation in the presence of several spatially-related variables. The disadvantage of univariate simulation methods compared to their multivariate counterparts is that they cannot take into account the relationship between different variables. MAF is a strong and relevant method used to accomplish this purpose as it is capable of carrying out joint simulation of multiple variables [26, 27]. MAF is a modified version of principal component analysis (PCA), first used in a remote sensing study [28]. Later, in [29], this method was applied in geostatistical modeling. MAF has also been integrated with direct block simulation algorithms and used in industrial projects [30-32]. In another study, MAF was applied in combination with ordinary kriging to estimate the variation in grade values [33]. In another research work, MAF was used to model the mineralization controlling factors for Sary Gunay epithermal gold deposit, and the relationship between rock types and alteration was modeled and investigated by means of SIS [34]. Moreover, this method was applied for the detection of faults in an oil reservoir in order to differentiate the fault and non-fault zones [35]. In addition, in [36, 37], joint simulation of categorical and continuous variables was first developed with the aim of simulating ultimate grades via considering the occurrence probability of different rock types. Similar studies were conducted to simulate ultimate grades by considering the occurrence probability of various rock types and comparing the results with those of conditional simulation methods [36-39]. Risk analysis methods better differentiate ore-waste boundaries than do estimation and conditional simulation methods, which affect dilution and ore loss [40]. Also in [41], Monte Carlo simulation was used to produce random grade values from local cumulative distribution function (LCDF) of a selective mine unit (SMU). Comparing the geology of blocks with the simulated blocks presented different conditions of dilution and ore loss.

The main purpose of this study was to evaluate the internal dilution of the block model of Gohar Zamin iron ore deposit based on the exploratory drill hole data, joint simulation of assay data, and correction of simulated grades using the evaluated internal dilution. MAF was applied for joint simulation of assay variables, namely Fe, FeO, S, and P. In addition, the occurrence probability of each rock type was calculated by means of the SIS method. Eventually, dilution was determined per each block, and ultimate grades of Fe and FeO were calculated with regard to the values calculated for internal dilution.

2. Case study

2.1. Geological setting

Gohar Zamin iron ore deposit is located 50 Km SW of Sirjan, Kerman Province, SE Iran. With an estimated ore tonnage of 643 Mt, this mine is considered as one of the largest iron resources in Iran. The overall shape of the deposit is similar to a faulty mass in which the northern and southern ends of the deposit are close to the surface, while the central part is in the depth. The mineralization in this region is mainly magnetite that occurs within a series of metamorphic rocks with greenschist facies to amphibolite facies. Figure 1b demonstrates the map of rock type outcrops along the mine walls (March 2018). Iron mineralization occurs in metamorphic rocks. The region is affected by shears such that several faults and fractures have cut the rock units. The

mineralization zone is along the metamorphic schist layers with a thickness of 40 to 60 m. The major faults of the mine area are shown in Figure 1b. Generally, the region consists of a complex of metamorphic rocks related to the Sanandaj-Sirjan belt and the Kore-Sefid complex of Paleozoic age. The rock types of Gohar Zamin complex include (old to young, respectively): 1) ultramafic serpentine and metamorphic gabbro, 2) dolomitic and calcic marbles, 3) mica schist along with gneiss and amphibolite, 4) gneiss, and 5) a composition of calcic marbles, gneiss, mica schist, amphibolite, schist, and black quartz (Figures 1 a and b). Also the gangue minerals of the deposit are laminated minerals such as talc, chlorite, serpentine, forsterite, tremolite, amphibole, edenite, dolomite, and calcite.

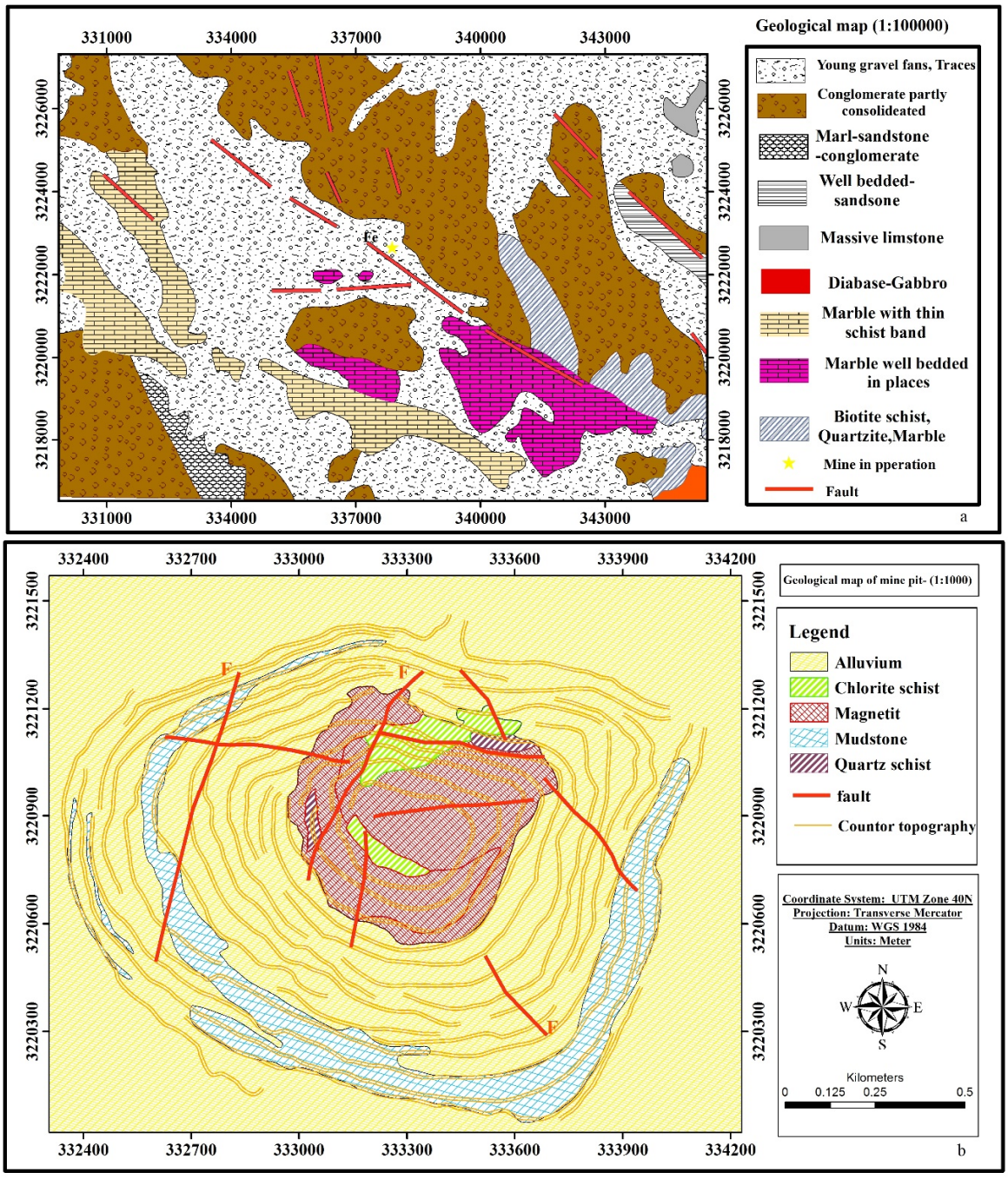

Figure 1. a) Geological map of the studied area (Scale-1:100.000); b) Geological map of the mine pit (Scale-1:1000).

2.2. Dataset

The mining operations are more concentrated in the northern part of the deposit, and evaluation of the internal dilution was carried out according to the data available from this region. The dataset consisted of 156 drill holes with the overall drilling of 37,500 m (north part of the deposit). In this work, 753 composite samples (each 6 m long) were collected from the drill hole core, and they included the assay data of Fe, FeO, S, and P. It should be mentioned that all these samples were gathered from the ore-containing regions. This data was deployed for joint simulation of the aforementioned variables using the MAF method. Other oxide variables like SiO_2, Al_2O_3, and MgO were not adequate in the dataset, and, therefore, they were ignored in this work. In order to assess internal dilution, the primary geological model of the deposit was created based on the first and the last occurrence of ore in each drill hole; internal dilution was evaluated within this model (Figures 2 a and b). Also the composite intervals of 2 m was considered for further modeling of rock types, leading to the extension of the dataset to include 2699 rock samples. Among these, 2281 samples were coded as ore and 418 others were coded as waste. Rock codes were composited based on geological lithology logs. The choice of 2 m for the composite of cores, determined based on the rock type and the geological log data with high resolution, was reliable and useful. The descriptive statistical analysis of the assay and lithological data is presented in Table 1. The grade and rock type simulations were conducted within a block model that was constant with the grid size of 10 × 10 × 15 m. Due to the fixed size of the block model in this mine, it was crucial to explore dilution, especially in the internal waste layer and margin boundary. Moreover, the data was also obtained from some blast holes that had been drilled in the north part of the deposit and contained lithological logs. Considering the lithological log of the blast holes, the dilution of each pattern was calculated based on the amount of ore and waste in the lithological log of the same pattern and then compared with the results of the assessed dilution in their corresponding block locations.

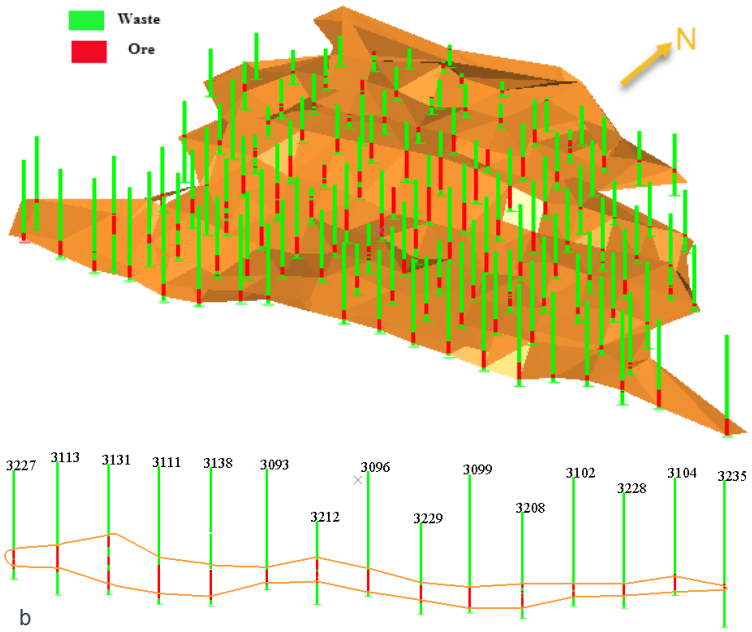

Figure 2. a) The simulated space for internal dilution of orebody #3 of the Gohar Zamin iron ore deposit. b) The boundary of simulated space area based on the first and last occurrence of iron in each drill hole.

Table 1. Descriptive statistics of continuous variables (assay data).

Variables	Number of data	Mean	Median	Variance	Minimum	Maximum	Skewness	Kurtosis
FeO	753	21.07	22.55	24.164	2	29	-1.558	2.214
Fe	753	52.95	55.30	91.032	11	66	-1.689	3.315
P	753	0.120	0.103	0.005	0.010	0.381	1.337	2.100
S	753	1.499	1.36	1.322	0.002	7.170	0.857	0.908

3. Methodology

3.1. Sequential indicator simulation (SIS)

The algorithm of SIS is similar to that of sequential Gaussian simulation (SGS). However, it simulates the categorical variables rather than the continuous ones [42, 43]. In this method, simulation is done based on the indicator variogram, and rock types are simulated by randomly drawing numbers from the cumulative distribution function (CDF) of different occurrence probabilities of rock facies. SIS can be employed where there is a lack of large-scale curvilinear features [44, 45]. Furthermore, this method is also capable of determining the approximate uncertainty that propagates through to the resulting numerical models [46, 47]. For the purpose of applying SIS, the rock types (Z_k) should be coded as follow:

$$\begin{cases} I(u;z_k)=1, \text{ in the presence of rock type k} \\ I(u;z_k)=0, \text{ in the absence of rock type k} \end{cases} \quad (1)$$

In this method, the simulation values are calculated using conditional probability distribution (CPD), which can be specified by calculating the conditional distribution of each rock facies using the neighborhood data for point u_α (Eq. 2) [46].

$$Prob\{z(u;zk)\} = \sum_{\alpha=1}^{n} \lambda\alpha(u;zk)\{i(u\alpha;zk)-mk\}+mk \quad (2)$$

where λ_α represents the kriging weights and m_k is the weight for each rock type that can be calculated as follows:

$$mk = \frac{\sum_{\alpha=1}^{n} W\,\alpha i(u\alpha;Zk)}{n} \quad (3)$$

where w_α corresponds to the weight of classified data. The algorithm of SIS is described as follows [48]:

1- Define a path that visits all locations that are to be simulated

2- Perform the following process for each location (u) along its path:

3- Retrieve the neighboring categorical conditioning data: z(uα), α = 1,..., n(u)

4- Convert each datum z(uα) into a vector of indicator data values: i(uα) = [i(uα, z1),..., i(uα, zK)]

5- Estimate the indicator random variable I (u, k) for each one of the K categories through solving a simple kriging system

6- After correction of order relation deviations, the estimated values i∗(u, k) = Prob∗(Z(u) =k|(n)) estimate the discrete conditional variable

7- Create the conditional probability density function (CPDF) of the categorical variable Z(u)

8- Draw a simulated category from CPDF and assign it as a datum at location u

9- End for

10- Reiterate these steps to develop another realization [48].

Figure 3 depicts a plot of CPDF for the rock type samples based on geological log in this area.

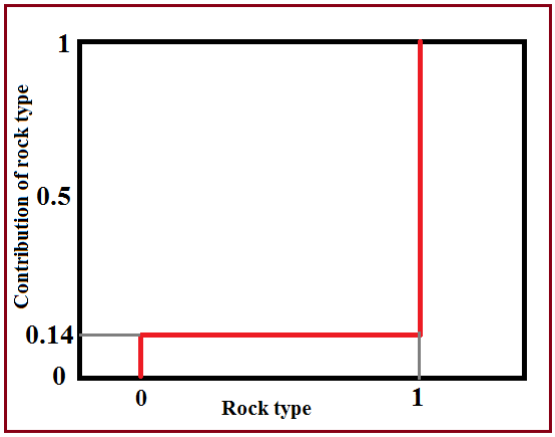

Figure 3. The conditional probability distribution calculated for a single point; the variables are simulated by randomly drawing a number from the distribution.

3.2. Minimum/maximum auto-correlation factor (MAF)

As mentioned earlier, the multivariate analysis methods, especially MAF, have been used in geostatistical studies in the past few years. MAF is a modified version of PCA in which the variables are de-correlated for all lag distances. In other words, by applying MAF, the variables are modeled spatially. Generally, MAF is an effective and practical tool in risk assessment when there are two or more variables. Two methods have been proposed for applying MAF, namely the model-based and data-driven methods. The model-based method considers the spatial relationships between the variables. In this method, the direct and cross-variograms of the variables (linear model of co-regionalization) are employed to transform the variables into spatially uncorrelated factors. On the other hand, the data-driven methods transform the variables into a

spatially uncorrelated factor regardless of the modeling of direct and cross-variograms of the variables. This work has utilized the data-driven approach. The MAF factors can be simulated separately and then back-transformed to the original space so that the correlations of the variables can be reproduced. The algorithm of data-driven MAF is presented as follows [26]:

1. Transform the data to normal score Gaussian distribution with a mean of zero and unit variance (Z_u)
2. Calculate the covariance-variance matrix B between variables
3. Decompose the covariance-variance matrix B into eigenvalues and the corresponding eigenvectors using the following equation:

$$B = Q^T \Lambda Q \rightarrow A = \Lambda^{-1/2} Q \quad (4)$$

where Λ is the diagonal matrix composed of eigenvalues and Q denotes the orthogonal matrix of eigenvectors.

4. Calculate the principal components using the following equation:

$$Y_{PCA}(u) = AZ(u) \quad (5)$$

5. Calculate matrix V through experimental variograms of Principle Component (PC) scores and further rotation of PCs by decomposing matrix V using Eq. 6. A detailed description of this matrix is given in [26].

$$V = Q_1^T \Lambda_1 Q_1 \quad (6)$$

where Λ_1 stands for a diagonal matrix of eigenvalues and Q_1 signifies an orthogonal matrix of eigenvectors extracted from matrix V.

6. Calculate the MAF factors based on Eq. 7:

$$F_{MAF}(u) = Q_1 Y_{PCA}(u) = Q_1 \Lambda^{-1/2} Q Z(u) = MZ(u) \quad (7)$$

7. Simulate the MAF factors
8. Back-transform the MAF simulated factors into primary variables using matrix M^{-1}
9. Back-transform the simulated variables into distributions of raw data.

The MAF factors have to be simulated discretely using the simulation methods such as SGS. As described earlier, the back-transformation of the MAF simulated factors to the original variables can be performed via matrix M^{-1}. In this matrix, the variables possess their special weights per each factor. Using the weights calculated by matrix M^{-1}, the mineralization factor can be inferred for further analysis.

4. Assessment of dilution

Any mixture of the ore with waste and unsolicited rock is called dilution. Due to dilution, the ore grade could be degraded so much that the whole extracted mass might be counted as a waste rock [49]. Dilution can best be defined as the proportion of waste tonnage to the total weight of ore and waste, as shown in Eq. 8 [2].

$$D(\%) = \frac{m_w}{m_W + m_O} \times 100 \quad (8)$$

where D is the percentage of dilution, m_w represents the tonnage of waste, and m_O refers to the tonnage of the extracted ore. Moreover, Eq. 8 can be re-phrased as Eq. 9, which is based upon the differing specific gravity (density) values of ore and waste rock. In this equation, ρ_W and ρ_O are, respectively, the specific gravity values of waste and ore, and V_W and V_O stand for the volumes of waste and ore in each block, respectively. The total volume of extracted rock is supposed to be 1 cubic meter for each block.

$$D = \left[\frac{\rho_W V_W}{\rho_W V_W + \rho_O V_O} \right] \quad (9)$$

$$V_O + V_W = 1 \quad (10)$$

The final variable grade of the total extraction material (ore and waste) can be calculated according to Eq. 11. Eq. 11 may be re-written in the form of Eq. 12 based on Eq. 9.

It should be noted that in those blocks with no proportion of waste, the results gained from both Eqs. 11 and 12 would be equal.

$$G_T = \left[\frac{m_W G_W + m_O G_O}{m_W + m_O} \right] \quad (11)$$

$$G_T = G_W D + G_O (1 - D) \quad (12)$$

where G_W and G_O are grades in waste and ore, respectively. Also m_W and m_O signify the respective tonnages of waste and ore. In the Gohar Zamin deposit, the grade measurement of waste samples was done solely for Fe and FeO. For this reason, it is not possible to calculate the ultimate

grades of the elements P and S in the samples. Based on waste samples, the average grades of Fe and FeO in the waste zone were 5 and 2 percent, respectively. For the present research work, the density of waste and ore samples was assumed to be equal to 2.65 and 4 gr/cm^3, respectively.

Different types of dilution are demonstrated in Figure 4. The internal dilution is due to the inclusion of gangue mineral with the orebody or the extraction of small low grade lenses [8]. This type of dilution can be investigated in veins with a small or large thickness within the block model. The constant size of the geologic block model can lead to the extraction of materials with different geological properties in the boundary regions. Therefore, in such regions, dilution can be considered geologic contact dilution (Figure 2).

In this work, the occurrence probability of different rock types was calculated via 100 SIS realizations. Afterwards, dilution was measured in each block based on Eq. 9. Additionally, the assay variables were simulated using 100 MAF realizations all over the ore body (Figure 2). Finally, the ultimate grade was achieved according to Eq. 12.

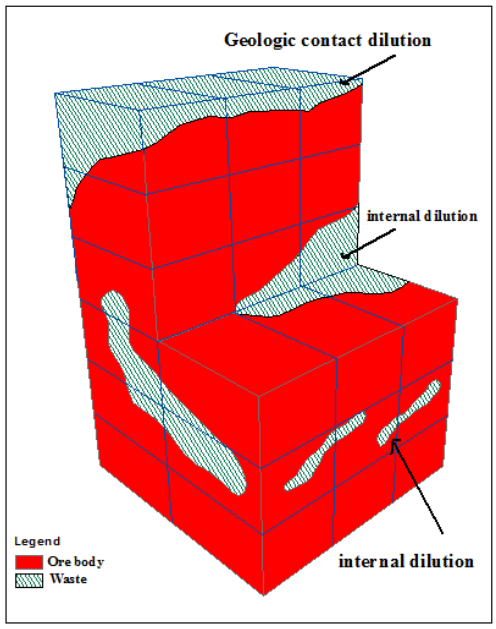

Figure 4. Different kinds of dilution occurring in mine blocks explored in this work.

5. Results and discussion

The main objective of this work was to evaluate the internal dilution of ore based on the geological data as well as the joint simulation of assay data, and subsequently, correcting the simulated grade values by considering the calculated values of internal dilution. Furthermore, calculating dilution helps determine the ultimate grade values for Fe and FeO per each block. Dilution was calculated using the volume proportion of waste for each block (Eq. 7). The analysis was carried out for a block model with a grid size of 10 × 10 × 15 m, which had been created using the data obtained from the drill holes in the northern part of the deposit. In the first step, the rock type simulation was carried out by means of the SIS method using the lithological data with composite intervals of 2 m, and the occurrence probability of different rock types was calculated for each block. Subsequently, internal dilution was measured per each block based on the ore-waste volume ratios and the density values assumed according to Eq. 9. In the next stage, the grade simulation of blocks was performed using 6-m-long composite samples of drill cores. Finally, the ultimate grades of Fe and FeO were determined according to Eq. 12. The average values for the calculated dilution were also compared with the experimental dilution considered by the mine experts.

5.1. Ore-waste modeling via SIS

Based on the geological logs of the drill hole data, the two types of rocks (ore-waste) were simulated by means of the SIS method. To this end, the indicator variogram of rock types was computed with regard to their anisotropy; the variogram model of the major direction is presented in Eq. 13. Subsequently, the simulation was conducted for 100 realizations, and the E-type map of the simulation was produced (Figure 5). The probability of ore occurrence was classified into four distinct categories for optimal visualization. The blocks with maximum probability of ore occurrence (0.75-1) are illustrated in red, and those with minimum probability of ore occurrence (0-0.25) are displayed in yellow (see Figure 5). The simulation maps of realizations 50 and 100 are also shown in Figure 6. The frequency histogram of the occurrence of different rock types is depicted in Figure 7. As demonstrated in this figure, 71 blocks were considered based on the results of the SIS method to be waste with the probability percentage of zero to 0.05. There were also 10,564 blocks among 28,152 ones that were considered to be ore with the probability percentage of 0.95 to 1.00. According to Figure 5, the occurrence probability of ore is smaller in the eastern and western parts of the deposit compared with the central parts.

$$\begin{aligned} &\Gamma(h) = 0.02 + 0.1Sph(690) + 0.11Sph(100), \\ &Az = 90 - Dip = 0 \end{aligned} \quad (13)$$

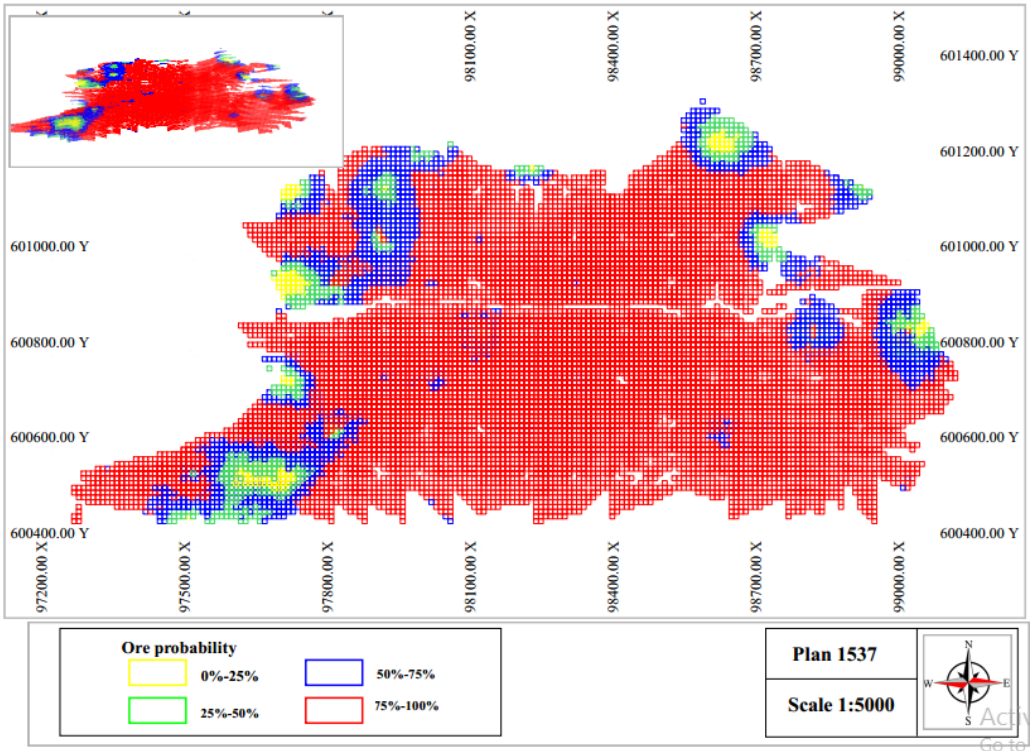

Figure 5. A plan section of E-type map of 100 simulation realizations related to level 1537 m; the probability of ore occurrence is lower in the east and west parts of the deposit.

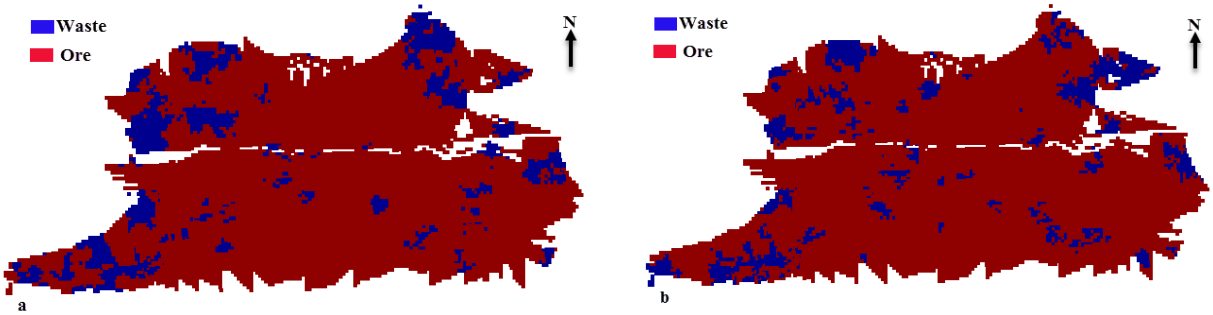

Figure 6. Simulation map of rock types a) realization 50, b) realization 100.

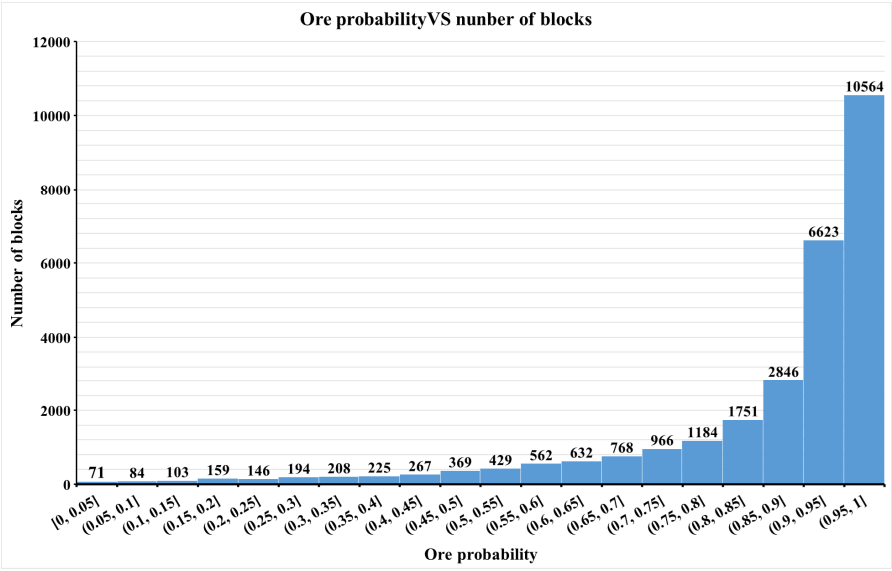

Figure 7. Frequency histogram of ore-waste occurrence probabilities.

5.2. Multivariate modeling of assay data

In this work, MAF was applied for the concurrent simulation of assay grade variables including Fe, FeO, P, and S. First, all variables of drill holes were normalized to Gaussian distribution, and the covariance variance matrix of the variables was produced (matrix B). According to matrix B, the maximum correlation belongs to the relationship between Fe and FeO, and the minimum degree of correlation is related to Fe and S. The rows and columns in matrix B correspond to the values for Fe, FeO, P, and S.

$$B = \begin{bmatrix} 1 & 0.736 & 0.035 & 0.173 \\ 0.736 & 1 & 0.026 & -0.057 \\ 0.035 & 0.026 & 1 & 0.069 \\ 0.173 & -0.057 & 0.069 & 1 \end{bmatrix}$$

In the next step, matrix B was decomposed to the matrices of eigenvalues and eigenvectors in order to produce PCs. Afterwards, matrix V was constructed by computing the experimental variograms of different PC scores. The variography process was conducted with different lag distances. The lag value of 25 m was extracted from the variograms in order to generate the following matrix (V):

$$V = \begin{bmatrix} 1.510 & -0.161 & -0.085 & -0.014 \\ -0.161 & 0.925 & -0.031 & -0.002 \\ 0.085 & -0.031 & 0.967 & -0.050 \\ 0.014 & -0.002 & -0.050 & 0.152 \end{bmatrix}$$

For further rotation of PCs, matrix V was decomposed to eigenvalues and eigenvectors, and the MAF factors were generated using values from matrix M (Eq. 7). The histograms of MAF scores are presented in Figure 8. All the produced factors demonstrate a normal distribution with a mean of almost zero and a variance of unit weight 1 (This data is summarized in Table 2). This fact can be taken as confirming the validity of MAF factors. Meanwhile, MAF factors have to be de-correlated spatially. In order to validate this issue, the cross-semi-variograms of factors were computed; all factors showed a good level of de-correlation in all lag distances (Figure 9).

After the de-correlation of MAF factors was ensured, all factors were simulated discretely by means of the SGS method. The variograms for each factor were calculated (Eq. 14), and simulation was employed for 100 realizations. The best simulation was chosen for a further analysis to better reproduce distribution of the original data. Finally, the simulated factors were back-transformed to the primary variables using matrix M^{-1}. This matrix provides the weights of each variable per each factor. All simulations were done for a block model of 10 × 10 × 15 m dimensions.

$$\begin{aligned} &\Gamma_{MAF1}(h) = 0.3Sph(690) + 0.7Sph(130), \\ &Az = 90 - Dip = 0 \\ &\Gamma_{MAF2}(h) = 0.3Sph(225) + 0.7Sph(105), \\ &Az = 0 - Dip = 0 \\ &\Gamma_{MAF3}(h) = 0.4Sph(577) + 0.6Sph(202), \\ &Az = 60 - Dip = 0 \\ &\Gamma_{MAF4}(h) = 0.4Sph(216) + 0.6Sph(780), \\ &Az = 55 - Dip = 0 \end{aligned} \quad (14)$$

$$M^{-1} = \begin{bmatrix} -0.940 & -0.24 & -0.025 & 0.339 \\ -0.921 & 0.062 & 0.091 & -0.373 \\ -0.056 & 0.364 & -0.925 & -0.095 \\ -0.098 & -0.885 & -0.432 & 0.143 \end{bmatrix}$$

One of the most significant advantages of MAF over univariate simulation is that it is capable of better reproducing correlations between variables. Therefore, this method was applied in this work in order to simulate the values for Fe and FeO within all blocks. The correlations between back-transformed variables and original variables were then computed in matrix H. In this matrix, the correlation coefficients of original variables are depicted in the upper diagonal half of the matrix, and the correlation coefficients of the back-transformed variables are shown in the lower diagonal half. It is evident that the results of the correlation coefficients of both methods are close to each other.

$$H = \begin{bmatrix} 1 & 0.736 & 0.035 & 0.173 \\ 0.793 & 1 & 0.026 & -0.057 \\ 0.097 & 0.112 & 1 & 0.069 \\ 0.075 & -0.082 & 0.021 & 1 \end{bmatrix}$$

Table 2. Descriptive statistics of MAF factors.

Variable	Number of data	Mean	Median	Variance	Minimum	Maximum	Skewness	Kurtosis
MAF1	753	-0.107	-0.0375	0.9970	-2.8401	2.9875	0.1300	-0.2100
MAF2	753	0.0078	0.0430	0.9870	-3.4124	2.4848	-0.1070	-0.1880
MAF3	753	-0.013	-0.0359	1.000	-3.1051	3.9082	0.1200	0.6680
MAF4	753	0.0113	0.1669	0.9998	-6.4878	4.1054	-1.7470	7.9130

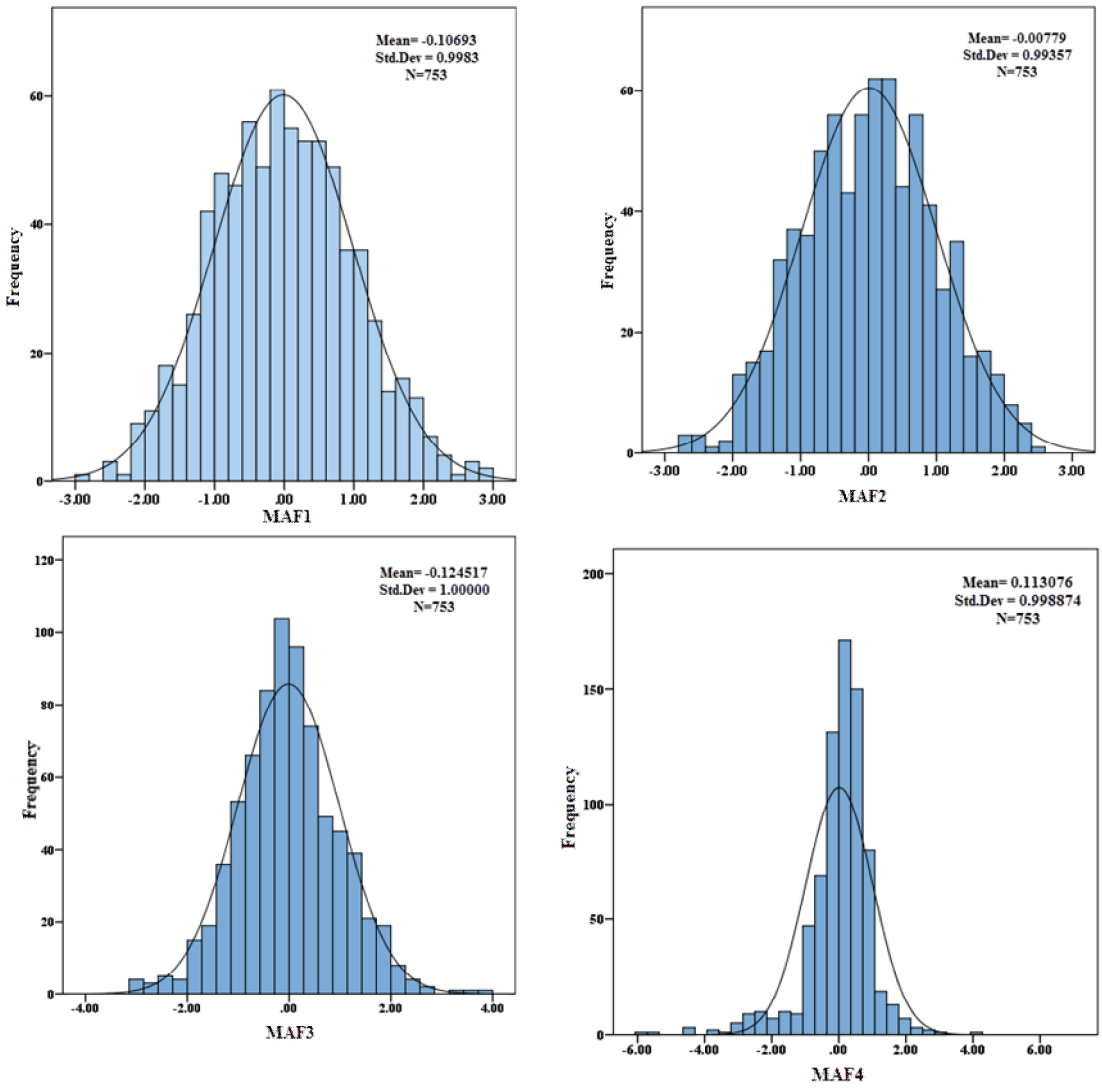

Figure 8. Histogram of MAF factors with a normal distribution.

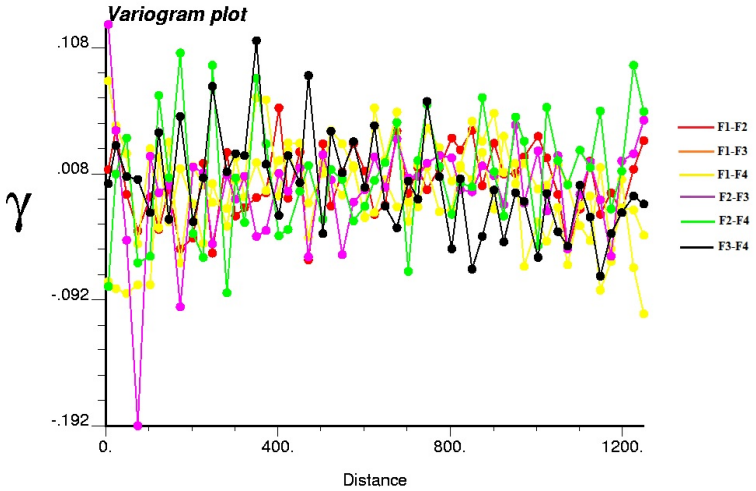

Figure 9. Experimental cross-semi-variograms of MAF factors; all factors are de-correlated spatially.

5.3. Evaluation of internal dilution in geological blocks

With regard to Eqs. 9 and 12, dilution and ultimate grade (denoted by (D) and (G_T), respectively) were approximated for each geological block using the simulated grades, the volume ratio of ore and waste for the block, as well as the known densities of ore and waste. It

was reasonably expected that the volume proportion of gangue mineral (waste) to ore in each supposed mining block should be in agreement with the geological structures located in that supposed block within the deposit. In other words, it is evident that the proportion of waste minerals to ore, as determined by SIS approximation, is bigger in areas where the non-ore-forming geological processes are dominant. Conversely, the proportion of waste decreases in blocks with less gangue mineral inclusion. For example, the results of SIS simulation for drill hole #3112 indicated that the ratio of ore to waste in the blocks was between 9% and 22% due to the presence of a waste layer with a thickness of 17 m (Figure 10). In this region, the probability of ore occurrence increases gradually to a maximum of 94% by moving westward toward the drill hole #3233; on the other hand, as one approaches the drill hole #3233, this probability decreases to 91% due to the presence of a waste layer of 2-m thickness. Moreover, in the border regions of the geological model, some parts of the blocks are located outside the boundaries (due to the constant dimensions of the blocks); also dilution increases dramatically due to the higher interference of waste, and hence, the lower probability of ore occurrence.

The calculated ultimate grades of the simulated block model are given in Figure 11. These grades were computed using Eq. 11. Calculating the final grade while considering dilution may lead the extracted block to end up in the waste dump rather than the ore processing plant. For example, for drill hole #3112, the ultimate grades of Fe and FeO were estimated as low as 10% while considering the 10% probability of ore occurrence. Therefore, the blocks have to be transported to the waste dump rather than the processing plant. Moreover, in the case of drill hole #3233, the probability of ore occurrence was 91% due to the presence of a waste layer with a 2-m thickness, and the ultimate grade of Fe decreased from 62.2% to 58.95% (Figure 11). The histogram of the calculated values for internal dilution of all blocks is depicted in Figure 12. It can be concluded that around 780 blocks suffer from lower grades due to the presence of internal-dilution values exceeding 50%. Naturally, the higher thickness of waste layers is also visible in the drill holes that are adjacent to blocks with a higher degree of calculated dilution. The locality of blocks with a dilution greater than 50% is shown in blue in Figure 13. Examining the lithological logs of drill holes that are adjacent to the points with a higher degree of calculated dilution reveals that the waste layers with a greater thickness could occur in these areas rather than other drill holes. It should be noted that the ratio of dilution was calculated by means of Eq. 9 based on the volumes and densities of ore and waste rock in each block.

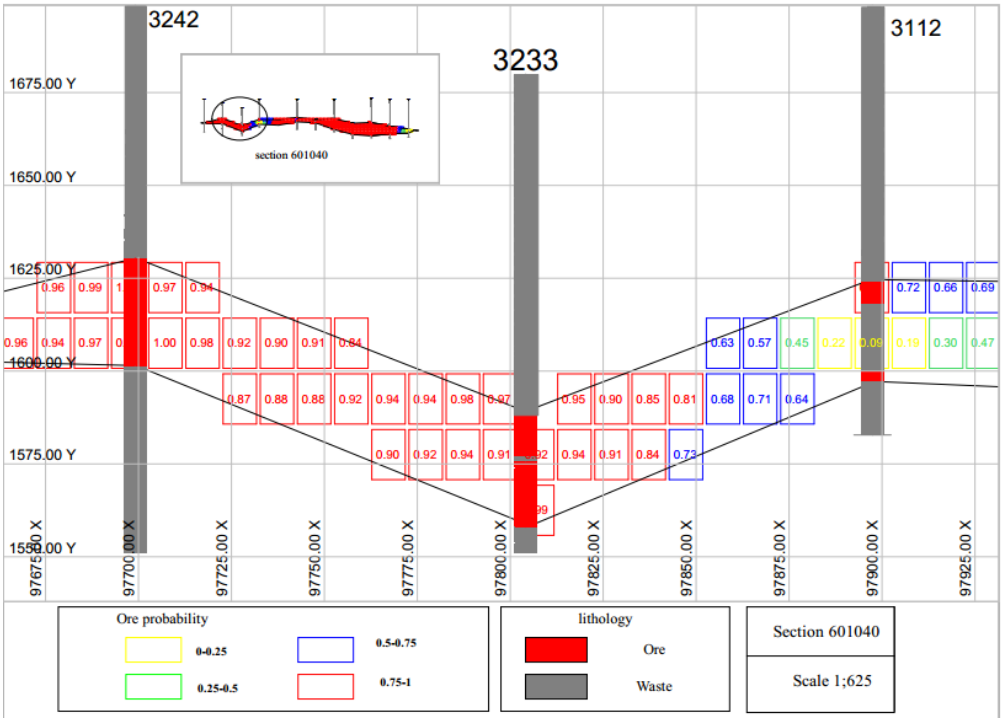

Figure 10. Probability of ore occurrence in geological blocks; western part of the vertical section 601040, Gohar Zamin mine.

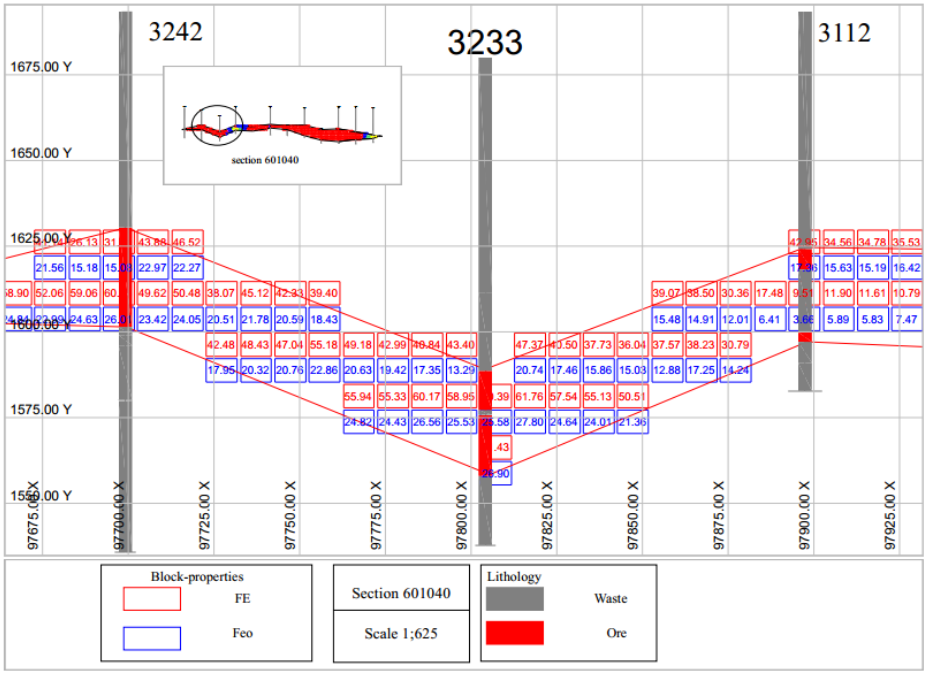

Figure 11. Total grades of Fe and FeO in the vertical section of 601040.

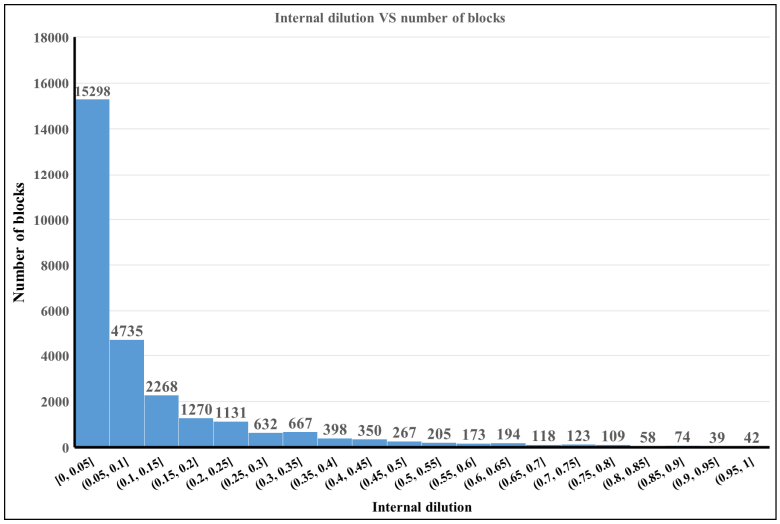

Figure 12. Frequency histogram of internal dilution within geological blocks.

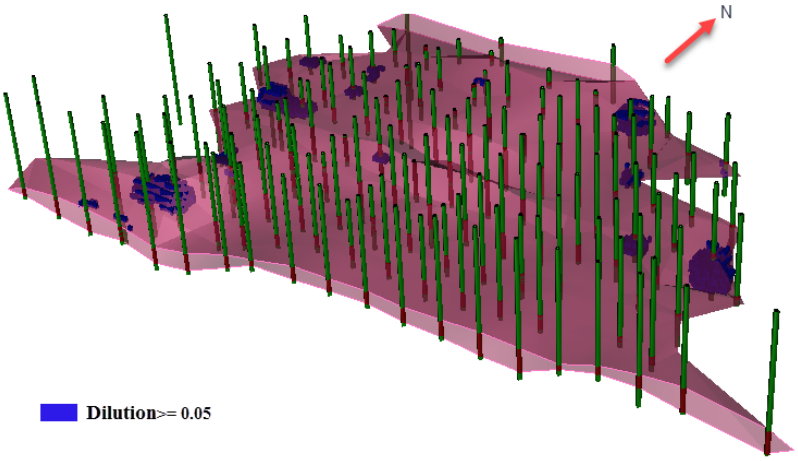

Figure 13. Internal dilution calculated within geological blocks; blocks with dilution over than 50% are presented in blue.

6. Validation

In the present work, validation of the results was investigated based on (1) the experimental dilution values measured in the mine site and (2) the lithological logs obtained from the blast holes.

6.1. Validation by experimental measurements of dilution

Based on calculating the internal dilution in each block (Eq. 9), the average value of the results for all blocks that have been defined in the simulation space for the northern part of Gohar Zamin iron ore mine is 10%, which is 2% more than the experimental dilution levels considered in the mine–these latter values are in the order of 7.5% to 8%. In this work, dilution was calculated independently for each block, and its impact on the reported final grade of Fe and FeO was also separately measured and reported. Comparing the mean final grade before and after applying the dilution calculated in all blocks shows a decrease of about 10% for these variables all over the mineral mass (Table 3).

Table 3. The average grade values for Fe and FeO calculated in both cases of considering dilution and ignoring dilution.

Variable	Average calculated grade before considering dilution (%)	Average calculated grade after considering dilution (%)	Grade reduction (%)
Fe	52.92	47.99	10%
FeO	21.02	18.99	10%

6.2. Validation via dilution values obtained from blast hole data

In order to validate the results of the presented model, one can also utilize the values of internal dilution in geological block models from the blast holes. These values are based on the percentage of ore and waste minerals observed in the lithological logs from the drilled blast holes. A blasting pattern for level 1567 of the mine is shown in Figure 14; the ore/waste simulation map obtained via the SIS method is also visible in the background. In this pattern, a total length of 612 m in the ore-containing region and 137 m in waste rocks was drilled. Consequently, the dilution value was calculated around 11% while considering the relevant densities for ore and waste rocks (Eq. 9).

Comparing the dilution values determined by blast hole lithological logs with the average simulated dilution values (in the order of 10%) reveals a high level of conformity and agreement. Moreover, there was an acceptable level of compatibility between the results of lithological simulations obtained from the drill hole data and the results of lithological logs of blast holes. This is especially the case for those blocks in which the probability of ore occurrence is lower than 25% and the lithology of blast hole is coded as waste. Nevertheless, there exist insignificant discrepancies between the simulation results and the lithological data, which can be attributed to the 2-m composite data used in the internal dilution space. Additionally, the disagreement between the exploratory drilling grid (with an average distance of 100 m between drill holes) and the blasting pattern can be regarded as another reason justifying the small discrepancies in the results. Figure 15 depicts another blasting pattern drilled on level 1567 of the mine. In this pattern, 94-98% of the blocks are simulated as ore. In order to investigate the validation of simulation results, the lithology logs of the blast holes were studied. It was observed that there existed inter-beds of waste rock with a thickness of 2 to 5 m in the lithological logs of the blast holes. Therefore, the overall length of ore and waste are 909 m and 106 m, respectively. The presence of waste inter-beds may reduce the probability of ore occurrence, which is estimated to be lower than 100%. Consequently, it can be concluded that the data from the blast holes well match the simulation results.

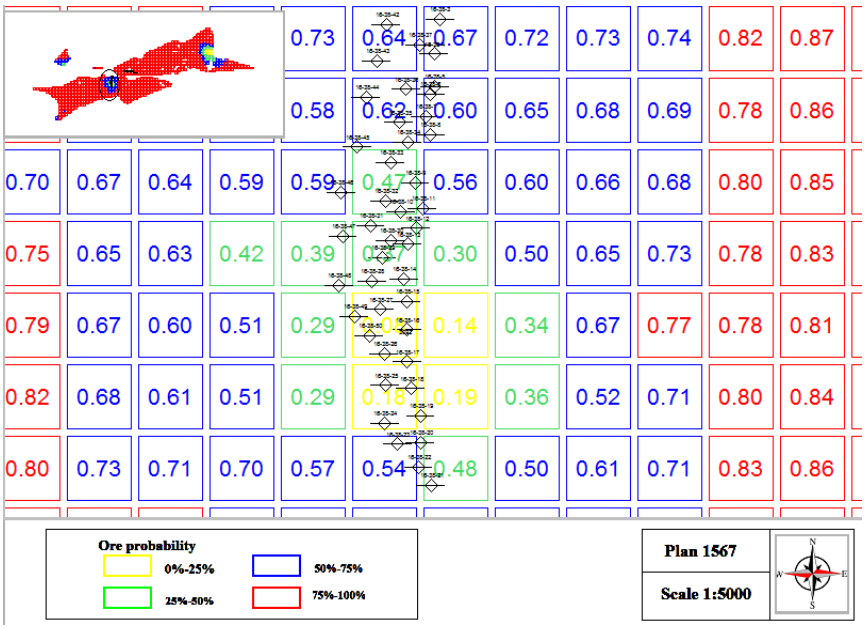

Figure 14. A selective blasting pattern drilled at plan 1567; the location of blast holes is shown within cycles.

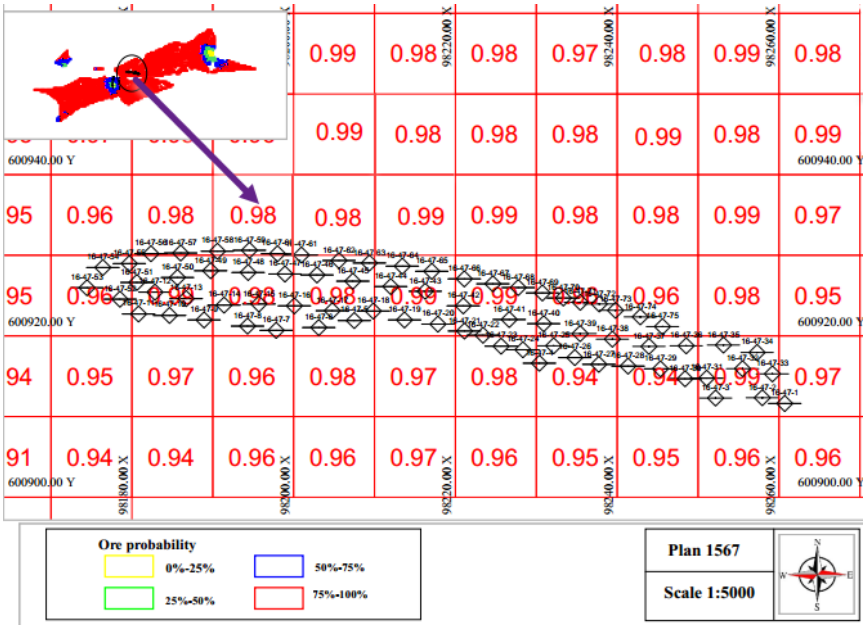

Figure 15. A blasting pattern drilled at plan 1567; the location of blast holes is shown within cycles.

7. Conclusions

Assessing the internal dilution has a significant role in mine production planning. In the present research work, the internal dilution of the Gohar Zamin iron ore deposit approximated the ultimate grades calculated for Fe and FeO. In order to achieve this goal, the lithological data of drill holes with the composite intervals of 2 m was coded as ore and waste based on geological logs; then the lithological model of the deposit was constructed using the sequential indicator simulation. In the next step, the volume proportions of ore and waste were calculated for each block and the relevant dilution value was determined. Furthermore, given the considerable importance of the accuracy of grade assessment for Fe and FeO in the later stages of long-term mine planning and dump management, these variables were simulated concurrently by means of a multivariate method, i.e. minimum/maximum auto-correlation factor. Finally, the ultimate grade values for Fe and FeO were corrected considering the applied dilution value calculated for each block in the previous stage. The results obtained indicated that the average value of internal dilution in all of the blocks was about 10%. Also a high degree of concurrence was observed between the calculated values of internal dilution and the

calculated probabilities of ore rock occurrence obtained from rock type simulation. Therefore, it can be concluded that the results obtained are reliable enough to be utilized in the next stages of mining such as long-term mine planning.

Acknowledgments
The authors would like to appreciate the Research and Development Unit of Gohar Zamin iron mine, especially Hamed Shamsedini, for their collaboration in collecting and accessing the data.

References

[1]. Popov, G.N. (1971). The working of mineral deposits: Mir Publishers.

[2]. Pakalnis, R., Poulin, R. and Vongpaisal, S. (1995). Quantifying dilution for underground mine operations. Paper presented at the Annual meeting of the Canadian Institute of Mining, Metallurgy and Petroleum, Halifax.

[3]. Pakalnis, R., Poulin, R. and Hadjigeorgiou, J. (1996). Quantifying the cost of dilution in underground mines. Paper presented at the International Journal of Rock Mechanics and Mining Sciences and Geomechanics Abstracts.

[4]. Annels, A.E. (2012). Mineral deposit evaluation: a practical approach: Springer Science & Business Media.

[5]. Henning, J.G. and Mitri, H.S. (2007). Numerical modelling of ore dilution in blasthole stoping. International Journal of Rock Mechanics and Mining Sciences. 44 (5): 692-703.

[6]. Saeedi, G., Rezai, B., Shareiar, K. and Oraee, K. (2008). Quantifying level of out-of-seam dilution for longwall mining method and its impact on yield of coal washing plant in Tabas coal mine. Paper presented at the Proceedings of the international seminar on mineral processing technology, Trivandrum, India.

[7]. Saeedi, G., Shahriar, K., Rezai, B. and Karpuz, C. (2010). Numerical modelling of out-of-seam dilution in longwall retreat mining. International Journal of Rock Mechanics and Mining Sciences. 47 (4): 533-543.

[8]. Ebrahimi, A. and Eng, P. (2013). The importance of dilution factor for open pit mining projects. Paper presented at the Proceedings of the 23rd World Mining Congress.

[9]. Yihong, L. and Weijin, Z. (1986). Reducing waste-rock dilution in narrow-vein conditions at tungsten mines in China. Mining Science and Technology. 4 (1): 1-7.

[10]. Planeta, S., Bourgoin, C. and Laflamme, M. (1990). The impact of rock dilution on undergroundmining: operational and financial considerations. Paper presented at the Proc. nnd CIM Annual General Meeting, Ottawa, Ontario.

[11]. Wang, J. (2004). Influence of stress, undercutting, blasting and time on open stope stability and dilution. University of Saskatchewan.

[12]. Jarosz, A. and Finlayson, R. (2003). GPS guidance system and reduction of open pit mining costs and revenue loss. Paper presented at the Spatıal Scıences, Inaugural Conference of Spatial Sciences Institute, Canberra, ACT, Australia.

[13]. Chugh, Y., Moharana, A. and Patwardhan, A. (2005). Dilution in underground coal mining in USA-impacts on production, processing and waste disposal. Paper presented at the International Conference on Mineral Processing Technology. New Delhi.

[14]. Mubita, D. (2005). Recent initiatives in reducting dilution at KonKola Mine, Zambia. Journal of the Southern African Institute of Mining and Metallurgy. 105 (2): 107-112.

[15]. Zarshenas, Y. and Saeedi, G. (2016). Risk assessment of dilution in open pit mines. Arabian Journal of Geosciences. 9 (3): 209.

[16]. Talebi, H., Asghari, O. and Emery, X. (2014). Simulation of the lately injected dykes in an Iranian porphyry copper deposit using the plurigaussian model. Arabian Journal of Geosciences. 7 (7): 2771-2780.

[17]. Alabert, F.G. (1987). Stochastic imaging of spatial distributions using hard and soft information. Stanford University Press.

[18]. Journel, A.G. and Gomez-Hernandez, J.J. (1993). Stochastic imaging of the Wilmington clastic sequence. SPE Formation Evaluation. 8 (01): 33-40.

[19]. Journel, A. and Isaaks, E. (1984). Conditional indicator simulation: application to a Saskatchewan uranium deposit. Journal of the International Association for Mathematical Geology. 16 (7): 685-718.

[20]. Matheron, G., Beucher, H., De Fouquet, C., Galli, A., Guerillot, D. and Ravenne, C. (1987). Conditional simulation of the geometry of fluvio-deltaic reservoirs. Paper presented at the Spe annual technical conference and exhibition.

[21]. Le Loc'h, G., Beucher, H., Galli, A. and Doligez, B. (1994). Improvement in the truncated Gaussian method: combining several Gaussian functions. Paper presented at the Ecmor iv-4th european conference on the mathematics of oil recovery.

[22]. Armstrong, M., Galli, A., Beucher, H., Loc'h, G., Renard, D., Doligez, B. and Geffroy, F. (2011). Plurigaussian simulations in geosciences: Springer Science & Business Media.

[23]. Rahimi, H., Asghari, O. and Hajizadeh, F. (2018). Selection of optimal thresholds for estimation and simulation based on indicator values of highly skewed distributions of ore data. Natural Resources Research. 27 (4): 437-453.

[24]. Schetselaar, E. (2013). Mapping the 3D lithofacies architecture of a VMS ore system on a curvilinear-faulted grid: A case study from the Flin Flon mining camp, Canada. Ore Geology Reviews. 53: 261-275.

[25]. Roldão, D., Ribeiro, D., Cunha, E., Noronha, R., Madsen, A. and Masetti, L. (2012). Combined use of lithological and grade simulations for risk analysis in iron ore, Brazil Geostatistics Oslo 2012 (pp. 423-434): Springer.

[26]. Rondon, O. (2012). Teaching aid: minimum/maximum autocorrelation factors for joint simulation of attributes. Mathematical Geosciences. 44 (4): 469-504.

[27]. Tajvidi, E., Monjezi, M., Asghari, O., Emery, X. and Foroughi, S. (2015). Application of joint conditional simulation to uncertainty quantification and resource classification. Arabian Journal of Geosciences. 8 (1): 455-463.

[28]. Switzer, P. (1985). Min/max autocorrelation factors for multivariate spatial imagery. Computer science and statistics.

[29]. Desbarats, A. and Dimitrakopoulos, R. (2000). Geostatistical simulation of regionalized pore-size distributions using min/max autocorrelation factors. Mathematical Geology. 32 (8): 919-942.

[30]. Boucher, A. and Dimitrakopoulos, R. (2009). Block simulation of multiple correlated variables. Mathematical Geosciences. 41 (2): 215-237.

[31]. Boucher, A. and Dimitrakopoulos, R. (2012). Multivariate block-support simulation of the Yandi iron ore deposit, Western Australia. Mathematical Geosciences. 44 (4): 449-468.

[32]. Lopes, J., Rosas, C., Fernandes, J. and Vanzela, G. (2011). Risk quantification in grade-tonnage curves and resource categorization in a lateritic nickel deposit using geologically constrained joint conditional simulation. Journal of Mining Science. 47 (2): 166-176.

[33]. Da Silva, C.Z. and Costa, J.F. (2014). Minimum/maximum autocorrelation factors applied to grade estimation. Stochastic environmental research and risk assessment. 28 (8): 1929-1938.

[34]. Ghane, B. and Asghari, O. (2017). Modeling of mineralization using minimum/maximum autocorrelation factor: case study Sury Gunay gold deposit NW of Iran. Geochemistry: Exploration, Environment, Analysis, geochem2016-453.

[35]. Shakiba, S., Asghari, O., Khah, N.K.F., Zabihi, S.S. and Tokhmechi, B. (2015). Fault and non-fault areas detection based on seismic data through min/max autocorrelation factors and fuzzy classification. Journal of Natural Gas Science and Engineering. 26: 51-60.

[36]. Emery, X. and Gonzalez, K.E. (2007). Incorporating the uncertainty in geological boundaries into mineral resources evaluation. JOURNAL-GEOLOGICAL SOCIETY OF INDIA. 69 (1): 29.

[37]. Emery, K. (2007). Probabilistic modelling of lithological domains and it application to resource evaluation. Journal of the Southern African Institute of Mining and Metallurgy. 107 (12): 803-809.

[38]. Emery, X. and Silva, D.A. (2009). Conditional co-simulation of continuous and categorical variables for geostatistical applications. Computers & Geosciences. 35 (6): 1234-1246.

[39]. Talebi, H., Asghari, O. and Emery, X. (2015). Stochastic rock type modeling in a porphyry copper deposit and its application to copper grade evaluation. Journal of Geochemical Exploration. 157: 162-168.

[40]. Haylett, M.E., Weeks, A., Matthews, G.D. and Khosrowshahi, S. (2014). Ore block design in narrow vein gold deposits – estimate or simulate?. Paper presented at the Ninth International Mining Geology Conference, Melbourne.

[41]. Ribeiro, D., Costa, J.F.C.L., Vidigal, M. and Roldão, D. (2009). Predicting Iron Ore Losses and Dilution Factors Using Conditional Simulations. Paper presented at the Iron Ore Melbourne.

[42]. Bierkens, M. and Burrough, P. (1993). The indicator approach to categorical soil data. Journal of Soil Science. 44 (2): 361-368.

[43]. Goovaerts, P. (1996). Stochastic simulation of categorical variables using a classification algorithm and simulated annealing. Mathematical Geology. 28 (7): 909-921.

[44]. Yin, Y. (2013). A new stochastic modeling of 3-D mud drapes inside point bar sands in meandering river deposits. Natural Resources Research. 22 (4): 311-320.

[45]. Nejadi, S. and Leung, J.Y. (2015). Estimation of facies boundaries using categorical indicators with P-Field simulation and ensemble Kalman filter (EnKF). Natural Resources Research. 24 (2): 121-138.

[46]. Deutsch, C.V. (2006). A sequential indicator simulation program for categorical variables with point and block data: BlockSIS. Computers & Geosciences. 32 (10): 1669-1681.

[47]. Olea, R.A. and Luppens, J.A. (2012). Sequential simulation approach to modeling of multi-seam coal deposits with an application to the assessment of a Louisiana lignite. Natural Resources Research. 21 (4): 443-459.

[48]. Remy, N., Boucher, A. and Wu, J. (2009). Applied geostatistics with SGeMS: a user's guide: Cambridge University Press.

[49]. Rossi, M.E. and Deutsch, C.V. (2013). Mineral resource estimation: Springer Science & Business Media.

ارزیابی ترقیق داخلی بر اساس شبیه‌سازی چند متغیره با استفاده از داده‌های گمانه‌های اکتشافی

ایمان معصومی[۱]، غلامرضا کمالی[۱] و امید اصغری[۲*]

۱- بخش مهندسی معدن، دانشگاه شهید باهنر کرمان، ایران

۲-آزمایشگاه شبیه‌سازی و پردازش داده، دانشکده مهندسی معدن، پردیس دانشکده‌های فنی، دانشگاه تهران، ایران

ارسال ۲۰۱۸/۱۱/۳، پذیرش ۲۰۱۹/۱/۳

* نویسنده مسئول مکاتبات: o.asghari@ut.ac.ir

چکیده:

ترقیق بر اساس میزان تناژ باطله به مجموع تناژ ماده معدنی و باطله در هر بلوک تعریف می‌شود. پیش‌بینی میزان ترقیق داخلی بر اساس مرزهای زمین‌شناسی ماده معدنی و باطله در هر بلوک به طراحی‌های برنامه‌های بلندمدت واقعی مهندسان کمک می‌کند. در این پژوهش روشی برای محاسبه میزان ترقیق داخلی زمین‌شناسی معرفی و عیار نهایی هر بلوک بر اساس میزان ترقیق داخلی آن محاسبه شده است. در ابتدا داده‌های ورودی از گمانه‌های اکتشافی بر اساس لاگ زمین‌شناسی آن‌ها در دو دسته ماده معدنی و باطله کدگذاری شده است. با استفاده از شبیه‌سازی شاخص متوالی در ۱۰۰ تحقق، احتمال حضور ماده معدنی و باطله در هر بلوک مشخص و ترقیق بر اساس نسبت تناژ باطله به کل تناژ هر بلوک محاسبه شده است. از روش فاکتور خود همبسته کمینه- بیشینه برای شبیه‌سازی متغیرهای عیاری پیوسته استفاده و در پایان عیار نهایی هر بلوک برای متغیرهای آهن و اکسید آهن بر اساس ترقیق داخلی محاسبه شده، اعلام شده است. این روش برای معدن سنگ‌آهن گهر زمین بررسی و ترقیق محاسبه شده با این روش با ترقیق محاسبه شده بر اساس لاگ لیتولوژی چال‌های حفاری مطابقت خوبی را داشته است.

کلمات کلیدی: ترقیق داخلی، شبیه‌سازی زمین‌آماری، شبیه‌سازی شاخص متوالی، فاکتور خود همبسته کمینه- بیشینه، معدن سنگ‌آهن گهر زمین.